Synthesis and Evaluation of Dihydropyrroloquinolines That Selectively Antagonize P-Glycoprotein

Brian D. Lee, Zhanjiang Li, Kevin J. French, Yan Zhuang, Zuping Xia, and Charles D. Smith*

Department of Pharmacology, The Pennsylvania State University, College of Medicine, Hershey, Pennsylvania 17033

Received July 3, 2003

In a search for improved multiple drug resistance (MDR) modulators, we identified a novel series of substituted pyrroloquinolines that selectively inhibits the function of P-glycoprotein (Pgp) without modulating multidrug resistance-related protein 1 (MRP1). These compounds were evaluated for their toxicity toward drug-sensitive tumor cells (i.e. MCF-7, T24) and for their ability to antagonize Pgp-mediated drug-resistant cells (i.e. NCI/ADR) and MRP1-mediated resistant cells (i.e. MCF-7/VP). Cytotoxicity and drug accumulation assays demonstrated that the dihydropyrroloquinolines inhibit Pgp to varying degrees, without any significant inhibition of MRP1. The compound termed PGP-4008 was the most effective at inhibiting Pgp in vitro and was further evaluated in vivo. PGP-4008 inhibited tumor growth in a murine syngeneic Pgp-mediated MDR solid tumor model when given in combination with doxorubicin. PGP-4008 was rapidly absorbed after intraperitoneal administration, with its plasma concentrations exceeding the in vitro effective dose for more than 2 h. PGP-4008 did not alter the plasma distribution of concomitantly administered anticancer drugs and did not cause systemic toxicity as was observed for cyclosporin A. Because of their enhanced selectivity toward Pgp, these substituted dihydropyrroloquinolines may be effective MDR modulators in a clinical setting.

Introduction

Cancer chemotherapy often fails because of the development of multiple drug resistance (MDR) by tumor cells. A major mechanism of MDR is through the overexpression of energy-dependent, unidirectional transmembrane efflux pumps. The drug transporter, P-glycoprotein (Pgp), is a 170 kDa protein that belongs to the ATP-binding cassette superfamily of transporters.[1] Its biochemistry and pharmacology have been intensely studied for the past 25 years.[2−4] A series of homologous proteins termed multidrug resistance-related proteins (MRPs) have been discovered more recently, and these proteins share many pharmacological properties with Pgp.[5,6] The first described protein of this series, MRP1, is a 190 kDa protein that was identified in 1992 in a drug-resistant lung cancer cell line that does not express Pgp.[7] These transporters function by binding to drugs within the cell and releasing them to the extracellular space using energy from the hydrolysis of ATP.[8] Tumor cells that are exposed to cytotoxic compounds often overexpress these efflux pumps, which allows these cells to survive even in the presence of anticancer drugs.[9]

MDR affects patients with a variety of cancers, including leukemias and solid tumors such as breast, lung, and brain cancers. Overexpression of Pgp has been documented in a number of tumor types including acute leukemia and small-cell lung carcinoma, especially after the patient has received chemotherapy, indicating that this mechanism of MDR is clinically important.[3,10−13] Additionally, several studies have shown that Pgp expression may be a prognostic indicator in certain malignancies. For example, increased expression of Pgp in neuroblastoma and childhood sarcoma is associated with poor response to chemotherapy and decreased survival,[14] and breast cancer patients with Pgp-expressing tumors are three times more likely to fail chemotherapy than those patients with Pgp-negative tumors.[15] In contrast, although MRP1 is expressed in a high percentage of leukemias and solid tumors,[16] its overexpression is not consistently found in tumors. For example, MRP1 levels detected in normal and malignant hematopoietic cells were equivalent,[17,18] and the MRP1 levels in lung tumors were found to be lower than those in normal lung tissue.[19] The MRP1 mRNA levels in malignant melanoma,[20] acute lymphocytic leukemia,[21] or chronic lymphocytic leukemia[22] were not altered by chemotherapy, but did increase moderately in acute myelogenous leukemia.[18,21] Therefore, it seems that overexpression of Pgp activity is clinically more significant than elevation of MRP1 levels.

Because of the importance of Pgp in clinical oncology, an intensive search has developed for antagonists of these transport proteins.[23] These antagonists, often termed MDR modulators, function by blocking the transporter-mediated drug efflux so that a concomitantly administered anticancer drug can cause tumor cell death. Initial attempts to develop MDR modulators focused on verapamil and cyclosporin A.[4,24] These compounds demonstrate excellent in vitro reversal of MDR but failed to achieve clinical success due to their intrinsic toxicity and/or their alteration of the pharmacokinetics of the coadministered anticancer drugs.[2,25,26] These clinical results may reflect differences in tissue distribution between the transport proteins, Pgp and MRP1. Previous studies have shown that Pgp is expressed by certain types of secretory cells, including the

* To whom correspondence should be addressed: Penn State College of Medicine, Department of Pharmacology, H078, 500 University Drive, Hershey, PA 17033. E-mail: cdsmith@psu.edu. Phone: (717) 531-1672. Fax: (717) 531-5013.

10.1021/jm0303204 CCC: $27.50
Published on Web 02/10/2004

Table 1. Cytotoxicity and MDR Antagonism by Substituted Dihydropyrroloquinolines

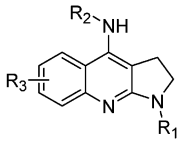

compd	R_1	R_2	R_3	Toxicity[a]	Pgp[b]	MRP1[c]	Pgp/MRP1
1	methyl	H	7-Br	94	1.3	1.6	0.8
2	methyl			12	1.6	1.0	1.6
3	methyl			22	5.6	1.0	5.6
4	methyl			39	1.8	1.4	1.3
5	methyl			28	3.2	1.2	2.7
6	methyl			30	6.0	1.2	5.0
7	methyl			51	4.1	1.2	3.4
8	methyl	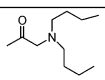		50	4.2	1.3	3.2
9	methyl	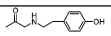		21	1.7	1.4	1.2
10	methyl			29	4.7	0.9	5.2
11	methyl	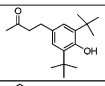		99	1.0	1.0	1.0
12	methyl			58	2.4	1.0	2.4
13	butyl	H	7-Br	98	1.1	1.0	1.1
14	cyclohexyl	H		97	0.8	0.6	1.3
15	cyclohexyl	H	7-Br	99	1.0	1.0	1.0
16	phenyl	H		52	2.7	1.1	2.5
17	3-chlorobenzyl			33	1.2	1.2	1.0
18	benzyl	H		47	3.1	1.0	3.1
19	benzyl	H	7-Br	94	1.7	1.3	1.3
20	benzyl	H	7-CH_3	98	0.7	1.0	0.7
21	benzyl	H	9-CH_3	77	1.6	1.7	0.9
22	benzyl	H	6,9-CH_3	81	1.5	1.2	1.3
23	benzyl	H	7,9-CH_3	49	3.6	1.4	2.6
24	benzyl			45	13	1.0	13
25	benzyl			29	12	0.9	13
26	benzyl			14	15	1.0	15
27	benzyl			0	18	1.1	16
28	benzyl	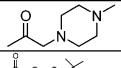		21	7.5	1.1	6.8
29	benzyl			50	13.2	1.2	11

[a] Toxicity is calculated as the percentage of MCF-7 cells killed by 10 μg/mL of the indicated compound. [b] The Pgp antagonism score = percentage of NCI/ADR cells surviving in the absence of vinblastine/percentage of NCI/ADR cells surviving in the presence of vinblastine. [c] The MRP1 antagonism score = percentage of MCF-7/VP cells surviving in the absence of vincristine/percentage of MCF-7/VP cells surviving in the presence of vincristine.

capillary endothelial cells of the brain and testis, and by cells within the pancreas, kidney, liver, and gastrointestinal tract.[22,27] Conversely, mRNA of MRP1 has been observed in virtually every type of tissue within the body[28] and is expressed in particular high concentration in peripheral blood mononuclear cells.[7,17,18,21,29]

The clinical significance of Pgp and its limited expression in normal tissues makes Pgp a target for the

Table 2. Reversal of Pgp- and MRP1-Mediated MDR by Dihydropyrroloquinolines

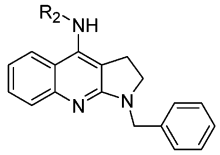

Compound	R_2	Toxicity IC_{50} (μM)	Antagonism at IC_{20} or less	
			Pgp	MRP
18	H	6.2	1.0	1.0
31	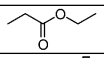	33	0.9	0.9
32		> 65	1.2	0.7
33	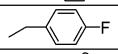	> 65	1.3	0.7
34	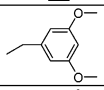	47	1.4	0.9
27	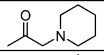	14	9.0	1.0
35 or PGP-4008		13	10.7	0.7
36	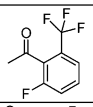	13	2.5	0.9
37	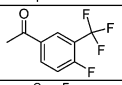	19	4.9	0.9
38		> 58	3.1	1.0

development of drugs to reverse MDR. It is likely that the lack of drug transporter-selectivity in early MDR modulators played a role in their ultimate failure. Therefore, we have hypothesized that improved selectivity of Pgp antagonists will provide more clinically effective chemotherapeutic agents.[30−32] Accordingly, some newer MDR modulators, including XR9576[33,34] and LY335979,[35] have improved Pgp selectivity and pharmacological properties.[30,31,36,37] To expand the portfolio of Pgp-selective MDR modulators, we screened a library of synthetic compounds and identified a series of dihydropyrroloquinolines that reverse Pgp-mediated MDR without antagonizing MRP1. We now describe the synthesis of substituted dihydropyrroloquinolines, structure−activity relationships for their effects on Pgp and MRP1, and the in vivo pharmacological properties of the most promising drug candidate, PGP-4008.

Results and Discussion

Identification of MDR-Reversing Dihydropyrroloquinolines. As with our previous studies,[30−32,38] we sought new inhibitors of Pgp and MRP1 using cell-based cytotoxicity assays with the following tumor cell lines: MCF-7, a drug-sensitive human breast adenocarcinoma line; NCI/ADR, a line selected for resistance to adriamycin that expresses high levels of Pgp without the overexpression of MRP1;[39] and MCF-7/VP, a subline of MCF-7 selected for resistance to etoposide in the presence of verapamil that expresses high levels of MRP1 without the overexpression of Pgp.[40] Cells were treated with a Pgp-substrate drug, vinblastine, or an MRP1-substrate drug, vincristine, either alone or in the presence of a test MDR modulator. Verapamil was used as the positive control and is highly effective at reversing both Pgp- and MRP1-mediated MDR in vitro.

Screening of approximately 11 000 compounds from a commercially available library was conducted at a final concentration of 10 μg/mL (15−25 μM) for the test compounds. This identified several chemotypes, including the dihydropyrroloquinoline heterocycle, with excellent promise as versatile scaffolds with which to study structure−activity relationships for inhibition of Pgp activity. The library contained 29 dihydropyrroloquinolines, whose biological activities are described in Table 1. The intrinsic cytotoxicity of the compounds is expressed as the percentage of MCF-7 cells killed by 10 μg/mL of each compound. It can be seen that these compounds have a wide range of toxicity, varying from 0% of cells killed by compound **27** to 99% of cells killed by compounds **11** and **15**. While toxicity toward cultured cells is a typical and desired property for cancer drugs, it is desirable that MDR modulators have low intrinsic toxicity. The ability of the dihydropyrroloquinolines in the screening library to reverse Pgp-mediated MDR is also indicated in Table 1. The Pgp antagonism score is calculated as the percentage survival of NCI/ADR cells treated with the compound alone divided by the percentage survival of NCI/ADR cells treated with the compound plus 50 nM vinblastine. Therefore, an antagonism score of 1.0 indicates inactivity of the test

Scheme 1

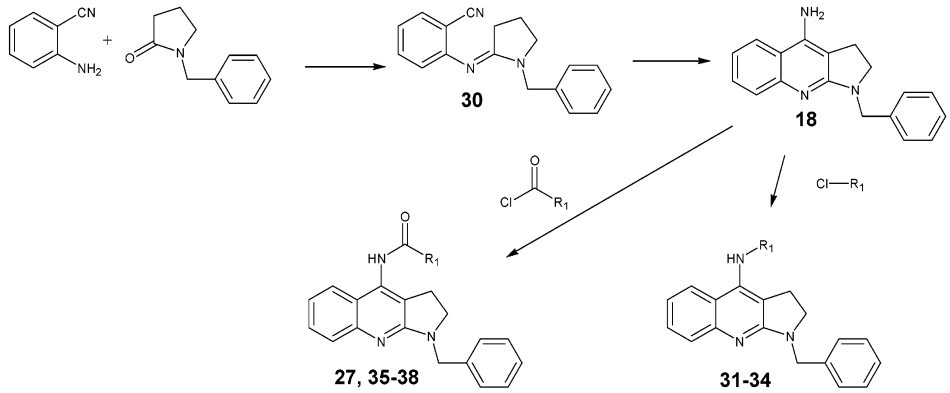

Table 3. Reaction Conditions, Yields, and Melting Points of Compounds **27** and **31**−**38**

	reaction conditions			
compound	catalyst	time (h)	yield (%)	mp (°C)
31	$(CH_3)_3COK$	1.5	61	132−134
32	$(CH_3)_3COK$	2	65	170−171
33	$(CH_3)_3COK$	3	80	167−169
34	$(CH_3)_3COK$	3	84	133−135
27	NaH	4	49	220−222
35 (PGP-4008)	NaH	3	52	157−159
36	NaH	2	55	189−191
37	NaH	1.5	45	195−197
38	NaH	2	53	160−162

compound, while larger antagonism scores indicate increasing activity. It is apparent that several of the dihydropyrroloquinolines inhibit Pgp function, with compounds **24**−**29** being particularly effective. The abilities of the compounds to reverse MRP1-mediated MDR are also indicated. The MRP1 antagonism score is calculated as the percentage survival of MCF-7/VP cells treated with the compound alone divided by the percentage survival of MCF-7/VP cells treated with the compound plus 1 nM vincristine, so that chemosensitization is indicated by a score greater than 1.0. In general, the dihydropyrroloquinolines had only marginal abilities to reverse MRP1-mediated MDR, so that several compounds are effective inhibitors of Pgp without inhibiting the action of MRP1. For example, compound **27** has a Pgp antagonism score of 18 whereas the MRP1 antagonism score is only 1.1. Compounds having a benzyl substitution at R_1 were more active toward Pgp than were corresponding compounds with methyl groups at that site, e.g. compound **27** compared with compound **7** and compound **29** compared with compound **11**. Additionally, increasing the size and/or hydrophobicity of the substituent at position R_2 enhanced activity toward Pgp, e.g. compound **27** > **26** > **25** = **24**. Thus, the initial screening indicated that bisubstituted dihydropyrroloquinolines provide a new and versatile chemotype for the development of Pgp-selective MDR antagonists.

Synthesis and In Vitro Evaluation of Novel Dihydropyrroloquinolines. A series of novel substituted dihydropyrroloquinolines, shown in Table 2, was synthesized as indicated in Scheme 1 and Table 3. 2-Aminobenzonitrile reacted with 1-benzyl-2-pyrrolidinone in the presence of phosphorus oxychloride and tin(IV) chloride to yield 2-(1-benzylpyrrolidin-2-ylidenemethyl)benzonitrile (**30**). Following the addition of lithium diisopropylamine−tetrahydrofuran complex, 1-benzyl-2,3-dihydro-1*H*-pyrrolo[2,3-*b*]quinolin-4-ylamine (**18**) was produced. Through alkylation and acetylation reactions, compounds **31**−**34**, **27**, and

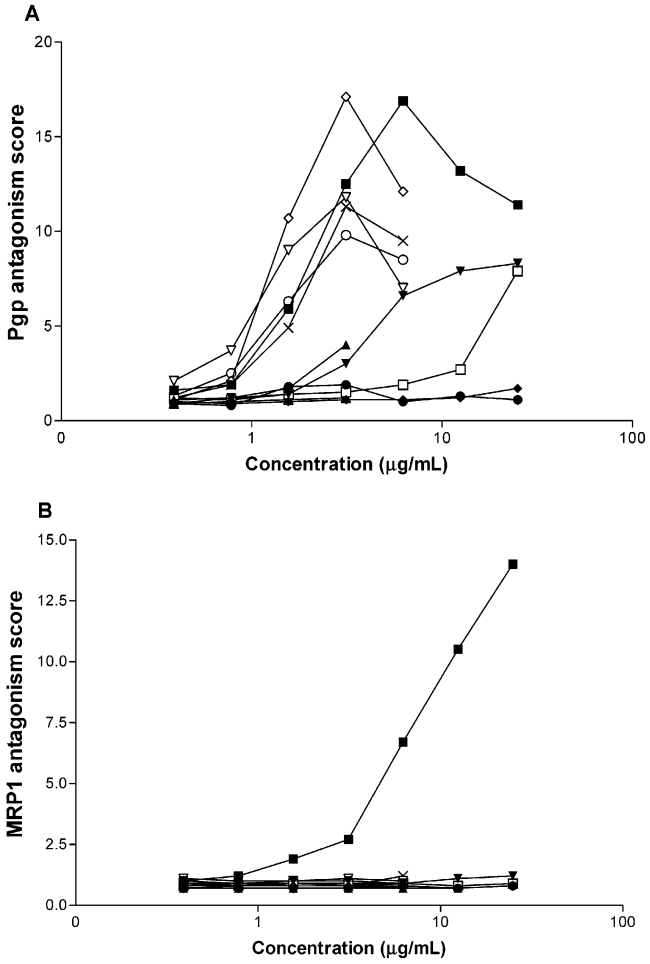

Figure 1. MDR reversal by dihydropyrroloquinolines. The reversal of Pgp- and MRP1-mediated MDR was assayed as described in the Experimental Section for the following compounds: verapamil (■); **18** (▲); **27** (▽); **31** (▼); **32** (◆); **33** (●); **34** (□); **35** (◇); **36** (○); **37** (×); **38** (△). (A) The Pgp Antagonism Score is calculated as the percentage of NCI/ADR cells surviving in the presence of 50 nM vinblastine/percentage of NCI/ADR cells surviving in the presence of vinblastine plus the indicated concentration of modulator. (B) The MRP1 Antagonism Score is calculated as the percentage of MCF-7/VP cells surviving in the presence of 1 nM vincristine/percentage of MCF-7/VP cells surviving in the presence of vincristine plus the indicated concentration of modulator.

Table 4. Cell Line- and Drug-Specificity of Verapamil and PGP-4008

		EtOH	verapamil		PGP-4008	
cell line	drug	IC_{50}	IC_{50}	RI[a]	IC_{50}	RI
T24	vinblastine (nM)	1.3 ± 0.3	0.5 ± 0.1	2.7	0.4 ± 0.1	3.8
	taxol (nM)	4.7 ± 0.5	3.0 ± 0.4	1.6	4.0 ± 0.6	1.2
	vincristine (nM)	4.8 ± 0.2	1.3 ± 0.2	3.7	2.2 ± 0.6	1.5
	cisplatin (μM)	6.7 ± 1.1	7.0 ± 0.8	1.0	5.8 ± 1.2	1.1
	5-Fluorouracil (μM)	77 ± 20	48 ± 6	1.6	29 ± 8	2.6
MCF-7	vinblastine (nM)	0.4 ± 0.1	0.3 ± 0.1	1.2	0.2 ± 0	1.8
	taxol (nM)	1.6 ± 0.3	1.4 ± 0.6	1.1	1.8 ± 0.1	0.9
	vincristine (nM)	0.6 ± 0.1	0.1 ± 0.1	4.6	0.4 ± 0.1	0.9
	cisplatin (μM)	16 ± 5	14 ± 4	1.1	19 ± 5	0.8
	5-Fluorouracil (μM)	49 ± 31	53 ± 20	0.9	30 ± 15	1.6
MCF7/VP (MRP1)	vinblastine (nM)	0.6 ± 0.1	0.2 ± 0	2.4	0.4 ± 0.1	1.3
	taxol (nM)	1.8 ± 0.4	1.6 ± 0.4	1.1	2.1 ± 0.4	0.8
	vincristine (nM)	7.5 ± 1.1	0.5 ± 0.2	15.0	7.3 ± 0.9	1.0
	cisplatin (μM)	8.5 ± 2.1	10.5 ± 3.2	0.8	11.3 ± 0.5	0.8
	5-fluorouracil (μM)	11 ± 1	12 ± 2	0.9	16 ± 3	0.7
NCI/ADR (Pgp)	vinblastine (nM)	110 ± 17	0.6 ± 0.1	173	3.1 ± 2.0	35
	taxol (nM)	2020 ± 810	19 ± 5	106	29 ± 5	70
	doxorubicin (μM)					
	vincristine (nM)	183 ± 14	3.7 ± 0.8	50	10.5 ± 1.1	18
	cisplatin (μM)	7.0 ± 0.9	6.3 ± 0.8	1.1	6.0 ± 0.5	1.2
	5-fluorouracil (μM)	181 ± 84	210 ± 99	0.9	175 ± 74	1.0
P388/ADR (Pgp)	vinblastine (nM)	28 ± 5	0.5 ± 0.1	61	0.5 ± 0.1	63
	taxol (nM)	1650 ± 470	5.0 ± 1.4	330	8.2 ± 2.9	202
	doxorubicin (μM)	26.7 ± 10.6	0.03 ± 0.01	1000	0.13 ± 0.09	200
	vincristine (nM)	150 ± 24	1.3 ± 0.5	112	5.0 ± 2.9	30
	cisplatin (μM)	2.1 ± 0.8	1.1 ± 0.3	2.0	1.1 ± 0.4	1.9
	5-fluorouracil (μM)	0.22 ± 0.04	0.30 ± 0.08	0.7	0.32 ± 0.08	0.7

[a] The reversal index (RI) is calculated as the ratio of the IC_{50} in the absence of modulator to the IC_{50} in the presence of modulator, so that larger values indicate increasing activity.

35−**38** were obtained. For in vivo studies described below, compound **35** or PGP-4008 was reacted with 2 equiv of hydrogen chloride in ether to obtain the corresponding HCl salt.

As detailed in Table 2 and Figure 1, the newly synthesized dihydropyrroloquinolines were found to exhibit a broad range of activity against Pgp, with PGP-4008 having a maximal activity equivalent to verapamil at a significantly lower concentration (Figure 1A). More importantly, none of the dihydropyrroloquinolines caused any significant antagonism of MRP1 (Figure 1B).

PGP-4008 was further characterized in a variety of cell lines with different cytotoxic drugs (Table 4). The reversal index (RI) was calculated as the ratio of the IC_{50} in the absence of modulator to the IC_{50} in the presence of modulator, so that larger values indicate increasing activity. PGP-4008 potentiated the cytotoxicity of Pgp substrate drugs (vinblastine, vincristine, and paclitaxel) toward cell lines that overexpress Pgp (NCI/ADR and P388/ADR), as indicated by the large reversal index. In contrast, PGP-4008 did not strongly affect the toxicities of these drugs toward non-Pgp-overexpressing cell lines (T24 and MCF-7), nor did they affect the toxicities of non-Pgp substrate drugs (cisplatin and 5-fluorouracil) toward any of the cell lines. PGP-4008 was not cytotoxic to any of the cell lines at doses up to 250 μM, thereby providing a large therapeutic index. In contrast with verapamil, the selectivity of PGP-4008 toward Pgp is again illustrated by the marked ability of verapamil to enhance the toxicity of vincristine to MRP1-overexpressing MCF7/VP cells, whereas PGP-4008 did not.

Additional studies have shown that PGP-4008 increases the accumulation of [^{3}H]paclitaxell and [^{3}H]vinblastine by NCI/ADR cells, without affecting the accumulation of these drugs by MCF-7 or MCF-7/VP cells (Figure 2). As with the cytotoxicity studies, the optimal effect of PGP-4008 was reached with doses below 2 μg/mL (5 μM). The modulatory effects of PGP-4008 observed in the cytotoxicity and drug accumulation assays are all consistent with selective antagonism of Pgp.

In Vivo Evaluation of PGP-4008. Initial in vivo experiments were hindered by the low solubility of PGP-4008; however, conversion to the HCl salt markedly improved its solubility. The therapeutic effects of PGP-4008·HCl were evaluated using a syngeneic solid tumor model consisting of JC murine mammary adenocarcinoma cells growing in Balb/c mice.[41] These cells are resistant to a variety of anticancer drugs because of their high level of expression of Pgp, and PGP-4008 effectively reverses this MDR phenotype. In these xenograft studies, tumors were allowed to grow to volumes of approximately 400 mm^3 before the animals were treated with saline (control), 5 mg/kg doxorubicin (a Pgp substrate), 100 mg/kg PGP-4008, or a combination of doxorubicin and PGP-4008. As shown in Table 5, tumor volumes in the control group increased 500% by day 15, while tumor volumes in animals treated with PGP-4008 alone or doxorubicin alone increased 500% and 300%, respectively. In contrast, tumors in animals treated with the combination of doxorubicin and PGP-4008 increased only 80% by day 15 ($p < 0.05$). There were no significant decreases in the weights of mice receiving the combination of PGP-4008 plus doxorubicin. This contrasts with the marked weight loss in animals treated with cyclosporin A, a nonselective MDR modulator.[41−43]

Pharmacokinetic studies of PGP-4008 were performed at the same dose as those used in the tumor studies. The plasma concentration profile of intraperitoneally administered PGP-4008 is shown in Figure 3, and the

Table 5. In Vivo Tumor Growth Inhibition by PGP-4008[a]

	day 1	day 5	day 9	day 12	day 15
control	380 ± 180	480 ± 130	1220 ± 500	1570 ± 560	2120 ± 800
doxorubicin	430 ± 180	520 ± 200	860 ± 280	1210 ± 530	1680 ± 720
PGP-4008	380 ± 190	470 ± 220	1030 ± 320	1280 ± 450	2000 ± 550
PGP-4008 + doxorubicin	390 ± 140	470 ± 140	*520 ± 110	*560 ± 160	*670 ± 170

[a] Tumor volumes (mm^3) are the average ± SD for 4−5 animals per group. *$p < 0.05$ compared to control.

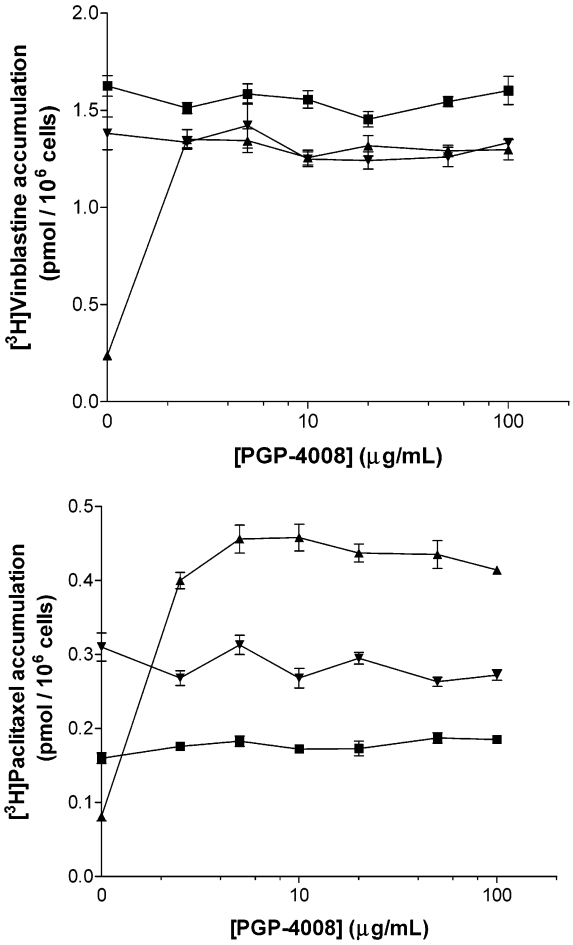

Figure 2. Effects of PGP-4008 on intracellular [^{3}H]drug accumulation. Intracellular accumulation of (A) [^{3}H]vinblastine and (B) [^{3}H]paclitaxel were performed using MCF-7 (■), NCI/ADR (▲), and MCF-7/VP (▼) cells and the indicated concentrations of PGP-4008 as described in the Experimental Section. Values represent the mean ± SD of triplicate samples in a representative experiment.

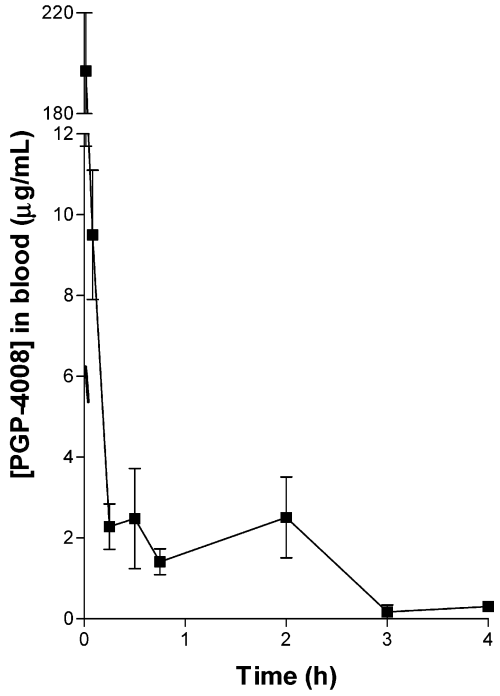

Figure 3. Pharmacokinetic profile of PGP-4008 in blood. PGP-4008 (100 mg/kg) was administered intraperitoneally to mice and blood samples were analyzed at the indicated times as described in the Experimental Section. Values represent the mean ± SD for triplicate samples in a representative experiment.

Table 6. Pharmacokinetic Parameters for PGP-4008

AUC	17.6 ± 1.4 μg × h/mL
AUMC	9.4 ± 5.2 μg × h^2/mL
A	440 ± 6 μg/mL
B	2.25 ± 0.36 μg/mL
k_α	49 ± 0.9 h^{-1}
k_β	0.58 ± 0.19 h^{-1}
$t_{1/2\beta}$	1.20 ± 0.39 h
k_{el}	35 ± 2.7 h^{-1}
V_{dss}	43 ± 15 mL
V_1	2.3 ± 0.3 mL
V_2	40.5 ± 7.4 mL
Cl_p	80.4 ± 6.4 mL/h

pharmacokinetic parameters are summarized in Table 6. Analysis of the concentration−time profile revealed that it best fits a two-compartment model, with rapid alpha-phase clearance and a beta-phase terminal half-life of 1.2 h. The highest concentration of PGP-4008 was observed at the earliest time point (1 min), indicating that PGP-4008 is rapidly absorbed into the systemic circulation from the intraperitoneal cavity. However, less than 1% of the peak concentration of PGP-4008 remained in the plasma after 4 h. The area under the concentration−time curve (AUC) for PGP-4008 was 17.6 μg·h/mL, with a clearance rate from the plasma (Cl_p) of 80.4 mL/h, corresponding to a large apparent volume of distribution (V_{dss} = 43 mL). The second compartment constitutes the majority of the volume of distribution of PGP-4008 (V_2 = 41 mL). Most importantly, however, is the fact that the maximum concentration in plasma (C_{max}, 197 μg/mL) was well above the in vitro effective dose of approximately 0.8 μg/mL. Furthermore, this effective concentration is maintained for at least 2 h, indicating that PGP-4008 is rapidly absorbed into the blood stream at therapeutically significant levels. Comparative studies in which PGP-4008 was administered intravenously indicated a bioavailability of 60% after intraperitoneal administration. Plasma distribution studies of vinblastine coadministered with PGP-4008 were also performed. As indicated in Figure 4, the clearance of [^{3}H]vinblastine was not altered by the presence of PGP-4008. This contrasts with the altered pharmacokinetic properties commonly seen with non-specific MDR modulators.[2]

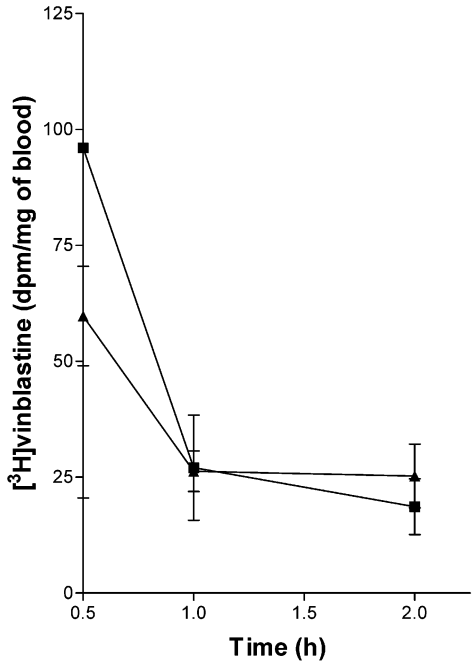

Figure 4. Effect of PGP-4008 on blood concentrations of [^{3}H]vinblastine. DMSO (■) or 100 mg/kg of PGP-4008 (▲) was administered intraperitoneally to mice followed by [^{3}H]vinblastine as described in the Experimental Section, and samples were analyzed at the indicated times for blood levels of [^{3}H]vinblastine as described in the Experimental Section. Values represent the mean ± SD for triplicate samples in a representative experiment.

Conclusions

We sought to develop MDR modulators that selectively antagonized Pgp to effectively potentiate the cytotoxicity of chemotherapeutic anticancer drugs toward resistant tumors. The dihydropyrroloquinoline heterocycle was chosen for its ease of synthesis and the presence of several substitution sites. Biological evaluation of several dihydropyrroloquinolines demonstrated their highly selective modulation of Pgp with maximal activity demonstrated by PGP-4008. In vivo testing of PGP-4008 demonstrated its efficacy for reversing Pgp-mediated MDR in a solid tumor model, its rapid systemic absorption, and its lack of interaction with a concomitantly administered chemotherapeutic agent. These results indicate the effectiveness of PGP-4008 in the reversal of Pgp-mediated MDR and its potential for clinical utility.

Experimental Section

Materials and Methods. Solvents were either purchased as "anhydrous" or "ACS grade" and stored over 4 Å molecular sieves. "Flash chromatography" refers to the method of Still et al.[44] and used Selecto Scientific silica gel (32−63 μm). Melting points were determined in an open capillary on a MelTemp II melting point apparatus and are uncorrected. Infrared spectra were measured on a Nicolet Avatar 360 FT-IR, and values are expressed in wavenumbers (cm^{-1}). ^{1}H and ^{13}C NMR spectra were obtained with a Bruker 200AM spectrometer. Chemical shifts are reported in ppm (δ) using tetramethylsilane as the reference and coupling constants (J) are reported in Hz. Mass spectra were obtained from Mass Consortium (San Diego, CA), and elemental analyses were performed by Midwest Microlab (Indianapolis, IN).

2-(1-Benzylpyrrolidin-2-ylideneamino)benzonitrile (30). To a solution of chloroform (25 mL) and tetrahydrofuran (25 mL) containing 1-benzyl-2-pyrrolidinone (5.16 g, 29.4 mmol) were added phosphorus oxychloride (5.2 mL) and tin(IV) chloride (1.0 mL). The mixture was stirred at room temperature for 1.5 h, before anthranilonitrile (3.3 g, 27.9 mmol) was added in portions and the mixture was stirred at 50 °C for 5 h. Ice-cold water (15 mL) was then added, and a 30% aqueous sodium hydroxide solution was further added to make a weak alkaline mixture. The organic solvent was removed under reduced pressure, and the residue was extracted with chloroform. The extract was dried over anhydrous sodium sulfate and condensed under vacuum. The crude product was purified by flash chromatography (chloroform:methanol, 100:1) to yield **30** (7.0 g, 91%) as slightly yellow needles, mp 59−61 °C; IR (KBr): 2217, 1628, 1439, 1279 cm^{-1}; ^{1}H NMR (DMSO-d_6): 7.06−7.69 (m, 9H), 4.83 (s, 2H), 3.46 (t, 2H), 2.60 (t, 2H), 2.10 (m, 2H); ^{13}C NMR ($CDCl_3$): 162.8, 156.3, 137.6, 133.7, 132.9, 128.7(2C), 128.3(2C), 127.4, 122.8, 121.7, 118.8, 105.9, 48.3, 47.3, 27.7, 19.6. Anal. Calcd for $C_{18}H_{17}N_3$ (275.35): C, 78.52; H, 6.22; N, 15.26. Found: C, 78.37; H, 6.20; N, 15.17.

1-Benzyl-2,3-dihydro-1*H*-pyrrolo[2,3-*b*]quinolin-4-ylamine (18). A solution of tetrahydrofuran (350 mL) containing **30** (37.6 g, 0.14 mol) under argon was cooled to −35 °C, and 1.5 M lithium diisopropylamine-tetrahydrofuran complex (233 mL, 0.35 mol) in cyclohexane was added dropwise. After the addition was complete, the temperature of the mixture was gradually raised to −10 °C, and ice-cold water (30 mL) was added dropwise. After the organic solvent was evaporated under reduced pressure, the residue was extracted with chloroform. The combined organic extracts were dried over anhydrous sodium sulfate and condensed under vacuum. The residue was dissolved in ethanol (15 mL), and crystals were precipitated, filtered, washed with cold ethanol, and dried under vacuum yielding 14.6 g (39%) of **18** as needles, mp 174−176 °C; IR (KBr): 3411, 3116, 1654, 1502, 1350, 756 cm^{-1}; ^{1}H NMR (DMSO-d_6): 7.01−7.93 (m, 9H), 6.05 (s, 2H), 4.60 (s, 2H), 3.37 (t, 2H), 2.87 (t, 2H); ^{13}C NMR ($CDCl_3$): 162.7, 149.3, 144.8, 138.8, 128.7(2C), 128.2(2C), 128.1, 127.2, 126.2, 121.8, 119.9, 117.6, 100.7, 48.4(2C), 23.3. Anal. Calcd for $C_{18}H_{17}N_3$ (275.35): C, 78.52; H, 6.22; N, 15.26. Found: C, 78.07; H, 6.07; N, 15.08.

General Procedure for the Synthesis of Compounds 31−34. To a solution of **18** (1 mmol) in tetrahydrofuran (15 mL) was added potassium *tert*-butoxide at 0 °C under nitrogen. After being stirred at room temperature for 1.5 h, the reaction mixture at −5 °C was added dropwise to a solution of corresponding alkyl chloride (1 mmol) in tetrahydrofuran (10 mL) using a syringe. The mixture was warmed to room temperature, stirred for 1.5−3 h, and then poured into water (50 mL) to precipitate a solid that was collected by filteration and dried under vacuum. The crude products were purified by flash chromatography (chloroform:methanol, 100:1) on silica gel to give the corresponding product (Table 3).

(1-Benzyl-2,3-dihydro-1*H*-pyrrolo[2,3-*b*]quinolin-4-ylamino)acetic Acid Ethyl Ester (31). Yield 61%; mp 132−134 °C; IR (KBr): 3410, 1745, 1620, 1502, 1215 cm^{-1}; ^{1}H NMR ($CDCl_3$): 7.16−7.72 (m, 9H), 4.77 (s, 2H), 4.25 (q, 2H), 3.51 (t, 2H), 3.49 (s, 2H), 3.11 (t, 2H), 1.34 (t, 3H); ^{13}C NMR ($CDCl_3$): 171.1, 157.4, 139.6, 137.1, 135.5, 132.1, 128.8(2C), 128.5(2C), 128.3, 127.3, 126.5, 124.5, 121.7, 120.5, 61.9, 48.7, 48.0, 26.1, 24.9, 14.6. Anal. Calcd for $C_{22}H_{23}N_3O_2$ (361.18): C, 73.11; H, 6.41; N, 11.63. Found: C, 73.04; H, 6.08; N, 11.90.

1-Benzyl-2,3-dihydro-1*H*-pyrrolo[2,3-*b*]quinolin-4-yl 3-fluorobenzylamine (32). Yield 65%; mp 170−171 °C; IR (KBr): 3400, 3063, 1622, 1504, 1217 cm^{-1}; ^{1}H NMR ($CDCl_3$): 7.00−8.15 (m, 13H), 4.73 (s, 2H), 4.19 (s, 2H), 3.21 (t, 2H), 2.45 (t, 2H); ^{13}C NMR ($CDCl_3$): 164.7, 162.5, 159.8, 149.8, 148.6, 137.8, 136.4, 133.5, 133.4, 130.4, 130.2, 128.6, 128.4, 128.2, 127.2, 126.6, 123.6, 121.7, 119.1, 115.4, 115.0, 54.5, 48.8, 47.8, 25.4. Anal. Calcd for $C_{25}H_{22}FN_3$ (383.46): C, 78.30; H, 5.78; N, 10.96. Found: C, 78.23; H, 5.32; N, 11.21.

1-Benzyl-2,3-dihydro-1*H*-pyrrolo[2,3-*b*]quinolin-4-yl 4-fluorobenzylamine (33). Yield 80%; mp 167−169 °C; IR (KBr): 3405, 1620, 1502, 1215 cm^{-1}; ^{1}H NMR ($CDCl_3$): 6.92−8.10 (m, 13H), 4.72 (s, 2H), 4.21 (s, 2H), 3.21 (t, 2H), 2.48 (t,

2H); ^{13}C NMR ($CDCl_3$): 165.5, 162.5, 160.6, 149.9, 148.5, 140.3, 137.8, 129.9, 128.7, 128.5, 128.2, 127.2, 126.7, 124.3, 123.5, 121.8, 119.1, 115.7, 115.3, 114.7, 114.2, 54.9, 48.9, 47.9, 25.5. Anal. Calcd for $C_{25}H_{22}FN_3$ (383.46): C, 78.30; H, 5.78; N, 10.96. Found: C, 78.73; H, 5.75; N, 11.08.

1-Benzyl-2,3-dihydro-1*H*-pyrrolo[2,3-*b*]quinolin-4-yl 3,5-dimethoxybenzylamine (34). Yield 84%; mp 133−135 °C; IR (KBr): 3420, 1621, 1509, 1218 cm^{-1}; ^{1}H NMR ($CDCl_3$): 6.57−8.15 (m, 12H), 4.71 (s, 2H), 4.13 (s, 2H), 3.67 (s, 6H), 3.23 (t, 2H), 2.56 (t, 2H); ^{13}C NMR ($CDCl_3$): 162.1, 160.6(2C), 149.5, 149.0, 141.4, 139.2, 1291, 128.4(2C), 128.2(2C), 127.2, 126.5, 123.7, 121.7, 121.5, 119.8, 106.6, 106.3, 99.6, 55.6(2C), 55.2, 48.8, 47.9, 25.5. Anal. Calcd for $C_{27}H_{27}N_3O_2$ (425.52): C, 76.21; H, 6.40; N, 9.87. Found: C, 76.23; H, 6.36; N, 9.50.

General Procedure for the Synthesis of Compounds 27 and 35−38. A solution of **18** (1 mmol) in DMF (10 mL) was added dropwise to a suspension of sodium hydride (1 mmol) in DMF (20 mL) at 0 °C under nitrogen. After 5 min, an acyl chloride was slowly added via syringe over a 20 min period maintaining a temperature of −5 °C. The reaction mixture was stirred at room temperature for 1−4 h (Table 3) and then filtered through silica gel. The solvent was removed under reduced pressure, and the residue was purified by flash chromatography (chloroform:methanol, 100:1) using silica gel to give the corresponding product (Table 3).

***N*-1-Benzyl-2,3-dihydro-1*H*-pyrrolo[2,3-*b*]quinolin-4-yl-2-piperidin-1-ylacetamide (27).** Yield 49%; mp 220−222 °C; IR (KBr): 3410, 1699, 1660, 1505 cm^{-1}; ^{1}H NMR (DMSO-d_6): 7.05−7.78 (m, 9H), 4.60 (s, 2H), 4.46 (s, 2H), 3.46 (m, 2H), 3.10 (m, 4H), 2.86 (t, 2H), 1.72 (m, 4H), 1.52 (m, 2H); ^{13}C NMR (DMSO-d_6): 168.6, 163.6, 149.6, 145.9, 139.5, 129.9(2C), 129.7(2C), 129.5, 128.6, 126.6, 122.7, 121.9, 118.4, 102.4, 60.6, 54.5(2C), 49.5(2C), 24.1, 23.9(2C), 22.7. Anal. Calcd for $C_{25}H_{28}N_4O$·HCl (437.02): C, 68.70; H, 6.70; N, 12.81. Found: C, 68.81; H, 6.43; N, 12.76.

***N*-1-Benzyl-2,3-dihydro-1*H*-pyrrolo[2,3-*b*]quinolin-4-yl-2-phenylacetamide (35 or PGP-4008).** Yield 52%; mp 157−159 °C; IR (KBr): 3431, 2959, 1690, 1665, 1507, 1310 cm^{-1}; ^{1}H NMR (DMSO-d_6): 7.29−8.37 (m, 14H), 5.17 (s, 2H), 3.93 (s, 2H), 3.77 (t, 2H), 2.97 (t, 2H); ^{13}C NMR (DMSO-d_6): 169.5, 156.5, 139.4, 137.2, 136.4, 135.1, 131.7, 129.9, 129.5(2C), 129.1(2C), 129.0(2C), 128.8(2C), 127.4, 125.3, 124.6, 123.6, 119.9, 118.8, 51.0, 50.5, 43.1, 25.8. Anal. Calcd for $C_{26}H_{23}N_3O$·H_2O (411.50): C, 75.88; H, 6.13; N, 10.21. Found: C, 76.29; H, 6.41; N, 9.82. The purity of **35** was confirmed to be >95% by HPLC analyses as described below.

***N*-(1-Benzyl-2,3-dihydro-1*H*-pyrrolo[2,3-*b*]quinolin-4-yl)-2-fluoro-6-trifluoromethylbenzamide (36).** Yield 55%; mp 189−191 °C; IR (KBr): 3427, 2933, 1691, 1628, 1119 cm^{-1}; ^{1}H NMR (DMSO-d_6): 7.35−8.25 (m, 12H), 5.02 (s, 2H), 3.66 (t, 2H), 2.98 (t, 2H); ^{13}C NMR (DMSO-d_6): 168.5, 165.3, 164.8, 161.2, 156.4, 148.4, 138.6, 136.4, 134.5, 131.1, 129.3(2C), 128.7(2C), 128.3, 124.1, 123.3, 122.5, 119.4, 119.1, 118.6, 116.3, 99.7, 50.3, 49.8, 23.8. Anal. Calcd for $C_{26}H_{19}F_4N_3O$ (465.44): C, 67.09; H, 4.11; N, 9.03. Found: C, 67.45; H, 4.19; N, 9.15.

***N*-(1-Benzyl-2,3-dihydro-1*H*-pyrrolo[2,3-*b*]quinolin-4-yl)-4-fluoro-3-trifluoromethylbenzamide (37).** Yield 45%; mp 195−197 °C; IR (KBr): 3435, 1691, 1626, 1375, 1118 cm^{-1}; ^{1}H NMR (DMSO-d_6): 7.25−8.62 (m, 12H), 4.95 (s, 2H), 3.37 (t, 2H), 3.00 (t, 2H); ^{13}C NMR (DMSO-d_6): 169.0, 165.0, 164.9, 161.2, 155.4, 147.9, 138.8, 136.0, 134.3, 131.0, 129.1, 128.7(2C), 128.2(2C), 124.1, 123.1, 122.5, 119.4, 119.1, 118.3, 116.7, 99.5, 50.8, 49.5, 23.5. Anal. Calcd for $C_{26}H_{19}F_4N_3O$ (465.44): C, 67.09; H, 4.11; N, 9.03. Found: C, 67.50; H, 4.05; N, 9.18.

***N*-(1-Benzyl-2,3-dihydro-1*H*-pyrrolo[2,3-*b*]quinolin-4-yl)-2,3,6-trifluorobenzamide (38).** Yield 53%; mp 160−162 °C; IR (KBr): 3430, 1689, 1378, 1119 cm^{-1}; ^{1}H NMR (DMSO-d_6): 7.33−8.31 (m, 11H), 5.14 (s, 2H), 3.84 (t, 2H), 3.13 (t, 2H); ^{13}C NMR (DMSO-d_6): 168.9, 165.3, 164.8, 161.2, 159.2, 159.1, 159.0, 138.2, 135.6, 132.3, 130.0, 129.4, 129.3, 125.9, 125.6, 124.5, 120.9, 120.5, 120.2, 119.6, 113.9, 113.4, 50.7, 49.8, 23.6. Anal. Calcd for $C_{25}H_{18}F_3N_3O$ (433.43): C, 69.28; H, 4.19; N, 9.69. Found: C, 69.28; H, 4.07; N, 9.62.

***N*-(1-Benzyl-2,3-dihydro-1*H*-pyrrolo[2,3-*b*]quinolin-4-yl)-2-phenylacetamide hydrochloride Salt (PGP-4008·HCl).** PGP-4008 (400 mg) was suspended in 1M HCl in ether (8 mL) and the mixture was stirred at room temperature for 12 h before the solvent was removed with nitrogen flushing. The residue was washed with 10% EtOAc in hexane twice and dried in vacuo to yield the yellowish solid, PGP-4008·HCl salt, 470 mg (Yield 99%). ^{1}H NMR (DMSO-d_6): 11.03 (s, 1H), 7.20−8.20 (m, 14H), 5.13 (s, 2H), 3.89 (s, 2H), 3.74 (t, 2H), 2.94 (t, 2H); ^{13}C NMR (DMSO-d_6): 168.5, 155.7, 138.4, 135.4, 134.2, 130.7, 129.1, 128.9 (2C), 128.6 (2C), 128.1 (2C), 128.0 (2C), 127.8, 126.4, 124.2, 123.6, 122.5, 119.0, 118.0, 50.0, 49.5, 42.2, 24.8.

In Vitro Cytotoxicity Assay. MCF-7 and NCI/ADR cells were obtained from the Division of Cancer Treatment of the National Cancer Institute.[39] MCF-7/VP cells were provided by Drs. Schneider and Cowan.[40] Cells were maintained in RPMI 1640 (Life Technologies, Inc., Rockville, MD) with L-glutamine containing 10% FBS and 50 μg/mL gentamicin at 37 °C and 5% CO_2. Cells were seeded into 96-well tissue culture dishes at approximately 20% confluency and allowed to recover and attach for 24 h. Cells were then treated in triplicate with varying concentrations of test modulators in the presence or absence of a cytotoxic drug for 48 h. The number of surviving cells remaining in each well was quantified with the sulforhodamine B (SRB) colorimetric assay.[45] Briefly, cells were washed with phosphate-buffered saline and fixed to the plate with 10% trichloroacetic acid. The cells were then washed with water and stained with 0.4% SRB in 1% acetic acid. Cells were then rinsed with 1% acetic acid, and 10 mM Tris buffer was added to dissolve the remaining SRB. The absorbance of each well was determined with a PerkinElmer HTS 7000 Plus BioAssay plate reader at a wavelength of 570 nm. The percentage of cells killed is calculated as the percentage decrease in SRB binding as compared with control cultures. Reversal of Pgp-mediated MDR was indicated if the compound enhanced the toxicity of vinblastine toward the NCI/ADR cells. The Pgp Antagonism Score was calculated as the percentage of surviving NCI/ADR cells in the absence of vinblastine divided by the percentage of surviving NCI/ADR cells in the presence of vinblastine. Control cultures included equivalent amounts of ethanol (1%, as the solvent control), which did not modulate the growth or drug-sensitivity of these cells. To assess the toxicity of the compounds toward drug-sensitive cells, the effects of the test modulators on the growth of drug-sensitive MCF-7 cells were determined by the same methods. Reversal of MRP1-mediated MDR was indicated if the compound enhanced the toxicity of vincristine toward MCF-7/VP cells. The MRP1 Antagonism Score was calculated as the percentage of surviving MCF-7/VP cells in the absence of vincristine divided by the percentage of surviving MCF-7/VP cells in the presence of vincristine.

In Vitro Drug Accumulation Assay. Cells were seeded in 24-well tissue culture dishes at approximately 25% confluency and allowed to recover and grow to near confluency, typically 3−4 days. Media was aspirated and replaced with serum-free media, and varying concentrations of PGP-4008 were added to the wells and cultures were incubated for 30 min at 37 °C. Approximately 0.1 μCi of [^{3}H]paclitaxel (75 Ci/mmol) or [^{3}H]vinblastine (7.3 Ci/mmol) (Moravek Biochemicals, Brea, CA) was then added per well, and the cultures were incubated for 60 min at 37 °C. Radioactive media was aspirated and cells were rapidly washed twice with ice-cold phosphate-buffered saline. Intracellular [^{3}H]drug was solubilized with 1% sodium dodecyl sulfate in water and quantified by liquid scintillation counting using UniverSol (ICN, Costa Mesa, CA) as previously described.[38]

In Vivo Toxicity Assay. Animal care and treatments were in accordance with guidelines and regulations of the Institutional Animal Care and Use Committee of The Penn State College of Medicine. Female Swiss-Webster mice (Charles River Laboratories, Wilmington, MA), 6−8 weeks old, were acclimated to their environment during quarantine for approximately 10 days before being released into the mouse

colony. Mice were housed (5 per cage) under 12 h light/dark cycles with food and water provided ad libitum. To evaluate the in vivo toxicity of PGP-4008, mice were injected in the intraperitoneal cavity with 20 mg/mL of PGP-4008 to give a total body concentration of 100 mg/kg (approximately 2.0 mg). Doses were administered once daily for 5 consecutive days, and mice were monitored for 2−3 weeks after the final injection.

In Vivo Tumor Growth Assay. Balb/c female mice (Charles River Laboratories, Wilmington, MA), 6−8 weeks old, were injected in the subcutaneous space of the right hind quarter with 10^6 JC cells (murine mammary adenocarcinoma, American Type Culture Collection CRL-2116, Manassas, VA) suspended in phosphate-buffered saline. After palpable tumor growth, approximately 2−3 weeks after injection, the tumor volumes were determined (day 1) using calipers measuring the length (L) and width (W) of the tumor. Tumor volumes were calculated using the equation: $(L \times W^2)/2$, and animals were randomized into four groups (five per group). Treatment was then administered on days 1, 5, and 9 and consisted of either intravenous administration of 50 mg/kg of cyclosporine injection USP[42] (Bedford Laboratories, Bedford, OH), with or without 5 mg/kg of doxorubicin hydrochloride (Sigma-Aldrich Co., St. Louis, MO); or intraperitoneal administration of 100 mg/kg of PGP-4008·HCl with or without doxorubicin hydrochloride. Tumor volumes were monitored until day 15 when the animals were euthanized, and treatment effects were compared by unpaired t-test with Welch correction using InStat (GraphPad Software, San Diego, CA).

Assay of the Pharmacokinetics of PGP-4008·HCl. Female Swiss-Webster mice, 6−8 weeks old, were injected intraperitoneally with 100 mg/kg of PGP-4008·HCl, and blood samples (0.7−0.8 mL) were obtained at times of 1−240 min (three animals per time point) by intracardiac puncture after anesthesia. Samples were immediately weighed and stored at −20 °C. For the analysis of PGP-4008 concentrations, 2-naphthol was added as an internal standard, and each sample was then precipitated with 12 mL ice-cold acetonitrile, vortexed vigorously, and centrifuged at 4000g for 15 min at 4 °C. The acetonitrile layers were then transferred to glass test tubes and evaporated to dryness under a stream of nitrogen at 45 °C. Samples were reconstituted in 0.2 mL of methanol and could be stored at −20 °C before they were analyzed by HPLC on a C8 reversed-phase Ultrasphere column (4 μm particle size, 4 × 250 mm, Beckman) with an isocratic mobile phase consisting of 60% 0.1% trifluoroacetic acid in water and 40% methanol at a flow rate of 1 mL/min. The recovery of the internal standard and PGP-4008 were monitored at 254 nm, with elution times of 7.9 and 14.3 min, respectively. Peaks were integrated and PGP-4008 concentrations were determined by using a standard curve, which was linear in all area ratios observed ($r^2 = 0.995$). The relative recoveries and coefficients of variation for the intraassay accuracy and precision were 92−106% and 4−8%, respectively. The quantification limit was 0.2 ng /mL. Interassay accuracy and precision were similar, with relative recovery and coefficient of variation values of 91−110% and 7−12%, respectively. All pharmacokinetic analyses were performed using the WinNonLin Standard software package (Pharsight) as follows: the area under the curve (AUC) was determined using the linear trapezoidal rule; the first-order elimination rate constant (k_{el}) was calculated using the slope of linearized log concentration plot; elimination half-life was determined by the formula $k_{el} = \alpha\beta/k_{21}$; and the bioavailability following intraperitoneal administration of PGP-4008 was determined by the following formula: $F = 100(AUC_{IP}/AUC_{IV})$.

Assay of Pharmacokinetic Interactions with Other Drugs. Female Swiss-Webster mice, 6−8 weeks old, were injected intraperitoneally with 100 mg/kg of PGP-4008·HCl as described above. Five minutes later, the mice were injected intravenously with [^{3}H]vinblastine (2 μCi/animal) at a dose of 10 mg/kg in a volume of 100 μL 0.9% saline. Blood samples (0.7−0.8 mL) were obtained at times of 30, 60, or 120 min (three animals per time point) by intracardiac puncture after anesthesia. For the analysis of [^{3}H]vinblastine concentrations, 0.1 mL of 100 mM EDTA and 0.3 mL of 30% H_2O_2 were added to decolorize the samples, followed by incubation for 1 h at 50 °C, cooling to room temperature, addition of 15 mL of Univer-Sol (ICN, Costa Mesa, CA), and quantification by liquid scintillation counting.

Acknowledgment. This work was supported by National Institute of Health Grant CA088243 (to C.D.S.).

Appendix

Abbreviations used: MDR, multiple drug resistance; MRP, multidrug resistance-related protein; Pgp, P-glycoprotein; RI, reversal index; SRB, sulforhodamine B.

References

(1) Juliano, R. L.; Ling, V. A surface glycoprotein modulating drug permeability in Chinese hamster ovary cell mutants. *Biochim. Biophys. Acta* **1976**, *455*, 152−162.
(2) Sikic, B.; Fisher, G.; Lum, B.; Halsey, J.; Beketic-Oreskovic, L.; et al. Modulation and prevention of multidrug resistance by inhibitors of P-glycoprotein. *Cancer Chemother. Pharmacol.* **1997**, *40*, S13−S19.
(3) Ling, V. Multidrug resistance: molecular mechanisms and clinical relevance. *Cancer Chemother. Pharmacol.* **1997**, *40*, S3−8.
(4) Tan, B. Multidrug resistance transporters and modulation. *Appl. Biochem. Biotechnol.* **2000**, *87*, 233−245.
(5) Grant, C. E.; Valdimarsson, G.; Hipfner, D. R.; Almquist, K. C.; Cole, S. P.; et al. Overexpression of multidrug resistance-associated protein (MRP) increases resistance to natural product drugs. *Cancer Res.* **1994**, *54*, 357−361.
(6) Kruh, G. D.; Chan, A.; Myers, K.; Gaughan, K.; Miki, T.; et al. Expression complementary DNA library transfer establishes mrp as a multidrug resistance gene. *Cancer Res.* **1994**, *54*, 1649−1652.
(7) Cole, S. P.; Bhardwaj, G.; Gerlach, J. H.; Mackie, J. E.; Grant, C. E.; et al. Overexpression of a transporter gene in a multidrug-resistant human lung cancer cell line. *Science* **1992**, *258*, 1650−1654.
(8) Horio, M.; Gottesman, M.; Pastan, I. ATP-dependent transport of vinblastine in vesicles from human multidrug-resistant cells. *Proc. Natl. Acad. Sci.* **1988**, *85*, 3580−3584.
(9) Kartner, N.; Riordan, J. R.; Ling, V. Cell surface P-glycoprotein associated with multidrug resistance in mammalian cell lines. *Science* **1983**, *221*, 1285−1288.
(10) Goldstein, L. J.; Galski, H.; Fojo, A.; Willingham, M.; Lai, S. L.; et al. Expression of a multidrug resistance gene in human cancers. *J. Natl. Cancer Inst.* **1989**, *81*, 116−124.
(11) Fojo, A. T.; Ueda, K.; Slamon, D. J.; Poplack, D. G.; Gottesman, M. M.; et al. Expression of a multidrug-resistance gene in human tumors and tissues. *Proc. Natl. Acad. Sci. U.S.A.* **1987**, *84*, 265−269.
(12) Bell, D. R.; Gerlach, J. H.; Kartner, N.; Buick, R. N.; Ling, V. Detection of P-glycoprotein in ovarian cancer: a molecular marker associated with multidrug resistance. *J. Clin. Oncol.* **1985**, *3*, 311−315.
(13) Ma, D. D.; Scurr, R. D.; Davey, R. A.; Mackertich, S. M.; Harman, D. H.; et al. Detection of a multidrug resistant phenotype in acute non-lymphoblastic leukaemia. *Lancet* **1987**, *1*, 135−137.
(14) van de Vrie, W.; Marquet, R. L.; Stoter, G.; De Bruijn, E. A.; Eggermont, A. M. In vivo model systems in P-glycoprotein-mediated multidrug resistance. *Crit. Rev. Clin. Lab Sci.* **1998**, *35*, 1−57.
(15) Trock, B. J.; Leonessa, F.; Clarke, R. Multidrug resistance in breast cancer: a meta-analysis of MDR1/gp170 expression and its possible functional significance. *J. Natl. Cancer Inst.* **1997**, *89*, 917−931.
(16) Nooter, K.; Westerman, A. M.; Flens, M. J.; Zaman, G. J.; Scheper, R. J.; et al. Expression of the multidrug resistance-associated protein (MRP) gene in human cancers. *Clin. Cancer Res.* **1995**, *1*, 1301−1310.
(17) Abbaszadegan, M. R.; Futscher, B. W.; Klimecki, W. T.; List, A.; Dalton, W. S. Analysis of multidrug resistance-associated protein (MRP) messenger RNA in normal and malignant hematopoietic cells. *Cancer Res.* **1994**, *54*, 4676−4679.
(18) Schneider, E.; Cowan, K. H.; Bader, H.; Toomey, S.; Schwartz, G. N.; et al. Increased expression of the multidrug resistance-associated protein gene in relapsed acute leukemia. *Blood* **1995**, *85*, 186−193.

(19) Thomas, G. A.; Barrand, M. A.; Stewart, S.; Rabbitts, P. H.; Williams, E. D.; et al. Expression of the multidrug resistance-associated protein (MRP) gene in human lung tumours and normal tissue as determined by in situ hybridisation. *Eur. J. Cancer* **1994**, *30A*, 1705−1709.
(20) Schadendorf, D.; Makki, A.; Stahr, C.; van Dyck, A.; Wanner, R.; et al. Membrane transport proteins associated with drug resistance expressed in human melanoma. *Am. J. Pathol.* **1995**, *147*, 1545−1552.
(21) Hart, S. M.; Ganeshaguru, K.; Hoffbrand, A. V.; Prentice, H. G.; Mehta, A. B. Expression of the multidrug resistance-associated protein (MRP) in acute leukaemia. *Leukemia* **1994**, *8*, 2163−2168.
(22) Leveille-Webster, C. R.; Arias, I. M. The biology of the P-glycoproteins. *J. Membr. Biol.* **1995**, *143*, 89−102.
(23) Robert, J.; Jarry, C. Multidrug resistance reversal agents. *J. Med. Chem.* **2003**, *46*, 4805−4817.
(24) Tsuruo, T.; Iida, H.; Tsukagoshi, S.; Y., S. Overcoming of vincristine resistance in P388 leukaemia in vivo and in vitro through enhanced cytotoxicity of vincristine and vinblastine by verapamil. *Cancer Res.* **1981**, *41*, 1967−1972.
(25) Kaye, S. B. Multidrug resistance: clinical relevance in solid tumours and strategies for circumvention. *Curr. Opin. Oncol.* **1998**, *10 Suppl 1*, S15−19.
(26) Sikic, B. I. Modulation of multidrug resistance: a paradigm for translational clinical research. *Oncology (Huntingt)* **1999**, *13*, 183−187.
(27) Endicott, J. A.; Ling, V. The biochemistry of P-glycoprotein-mediated multidrug resistance. *Annu. Rev. Biochem.* **1989**, *58*, 137−171.
(28) Zaman, G. J.; Versantvoort, C. H.; Smit, J. J.; Eijdems, E. W.; de Haas, M.; et al. Analysis of the expression of MRP, the gene for a new putative transmembrane drug transporter, in human multidrug resistant lung cancer cell lines. *Cancer Res.* **1993**, *53*, 1747−1750.
(29) Burger, H.; Nooter, K.; Sonneveld, P.; Van Wingerden, K. E.; Zaman, G. J.; et al. High expression of the multidrug resistance-associated protein (MRP) in chronic and prolymphocytic leukaemia. *Br. J. Haematol.* **1994**, *88*, 348−356.
(30) Lawrence, D. S.; Copper, J. E.; Smith, C. D. Structure−activity studies of substituted quinoxalinones as multiple-drug-resistance antagonists. *J. Med. Chem.* **2001**, *44*, 594−601.
(31) Smith, C. D. Azabicyclooctane compositions and methods for enhancing chemotherapy. US Patent 6,248,752, 2001.
(32) Smith, C. D.; Myers, C. B.; Zilfou, J. T.; Smith, S. N.; Lawrence, D. S. Indoloquinoxaline compounds that selectively antagonize P-glycoprotein. *Oncol. Res.* **2001**, *12*, 219−229.
(33) Martin, C.; Berridge, G.; Mistry, P.; Higgins, C.; Charlton, P.; et al. The molecular interaction of the high affinity reversal agent XR9576 with P-glycoprotein. *Br. J. Pharmacol.* **1999**, *128*, 403−411.
(34) Stewart, A.; Steiner, J.; Mellows, G.; Laguda, B.; Norris, D.; et al. Phase I trial of XR9576 in healthy volunteers demonstrates modulation of P-glycoprotein in CD56+ lymphocytes after oral and intravenous administration. *Clin. Cancer Res.* **2000**, *6*, 4186−4191.
(35) Dantzig, A. H.; Shepard, R. L.; Cao, J.; Law, K. L.; Ehlhardt, W. J.; et al. Reversal of P-glycoprotein-mediated multidrug resistance by a potent cyclopropyldibenzosuberane modulator, LY335979. *Cancer Res.* **1996**, *56*, 4171−4179.
(36) Roe, M.; Folkes, A.; Ashworth, P.; Brumwell, J.; Chima, L.; et al. Reversal of P-glycoprotein mediated multidrug resistance by novel anthranilamide derivatives. *Bioorg. Med. Chem. Lett.* **1999**, *9*, 595−600.
(37) Newman, M. J.; Rodarte, J. C.; Benbatoul, K. D.; Romano, S. J.; Zhang, C.; et al. Discovery and characterization of OC144−093, a novel inhibitor of P− glycoprotein-mediated multidrug resistance. *Cancer Res.* **2000**, *60*, 2964−2972.
(38) Smith, C. D.; Zilfou, J. T.; Stratmann, K.; Patterson, G. M.; Moore, R. E. Welwitindolinone analogues that reverse P-glycoprotein-mediated multiple drug resistance. *Mol. Pharmacol.* **1995**, *47*, 241−247.
(39) Fairchild, C. R.; Ivy, S. P.; Kao-Shan, C. S.; Whang-Peng, J.; Rosen, N.; et al. Isolation of amplified and overexpressed DNA sequences from adriamycin-resistant human breast cancer cells. *Cancer Res.* **1987**, *47*, 5141−5148.
(40) Schneider, E.; Horton, J. K.; Yang, C. H.; Nakagawa, M.; Cowan, K. H. Multidrug resistance-associated protein gene overexpression and reduced drug sensitivity of topoisomerase II in a human breast carcinoma MCF7 cell line selected for etoposide resistance. *Cancer Res.* **1994**, *54*, 152−158.
(41) Lee, B. D.; French, K. J.; Zhuang, Y.; Smith, C. D. Development of a syngeneic in vivo tumor model and its use in evaluating a novel P-glycoprotein modulator, PGP-4008. *Oncol. Res.* **2003**, *14*, 49−60.
(42) Watanabe, T.; Tsuge, H.; Oh-Hara, T.; Naito, M.; Tsuruo, T. Comparative study on reversal efficacy of SDZ PSC 833, cyclosporin A and verapamil on multidrug resistance in vitro and in vivo. *Acta Oncol.* **1995**, *34*, 235−241.
(43) Saito, T.; Zhang, Z. J.; Tokuriki, M.; Ohtsubo, T.; Shibamori, Y.; et al. Cyclosporin A inhibits the extrusion pump function of p-glycoprotein in the inner ear of mice treated with vinblastine and doxorubicin. *Brain Res.* **2001**, *901*, 265−270.
(44) Still, W. C. K., M.; Mitra, A. Rapid chromatographic techniques for preparative separation with moderate resolution. *J. Org. Chem.* **1978**, *43*, 2923−2924.
(45) Skehan, P.; Storeng, R.; Scudiero, D.; Monks, A.; McMahon, J.; et al. New colorimetric cytotoxicity assay for anticancer-drug screening. *J. Natl. Cancer Inst.* **1990**, *82*, 1107−1112.

JM0303204